phys. stat. sol. (a) **137**, 351 (1993)

Subject classification: 61.70 and 73.40; 78.45; S7.11

Department of Pure and Applied Physics, UMIST, Manchester[1]) *(a), Physics Department, University of Surrey, Guildford (b), and BNR Europe, Harlow (c)*

Studies of the Microstructure in Degraded Buried Heterostructure GaInAsP/InP Laser Diodes and Its Relation with the Lasing Threshold Current

By

U. BANGERT (a), A. J. HARVEY (b), A. R. GOODWIN (c), and A. T. R. BRIGGS (c)

Dedicated to Professor Dr. HELMUT ALEXANDER on the occasion of his 65th birthday

The microstructure of degraded GaInAsP/InP buried heterostructure laser diodes with low and high zinc-doping levels of the p-InP confining layer is investigated and correlated with the threshold current versus time curves. Dislocations, which were present before overstress life tests, initiate the degradation, whereas the microstructural characteristics and the degradation speed are controlled by the type of point defect initially present in the two kinds of laser diodes. These appear to be predominantly group-III vacancies and group-V interstitials in lasers with low zinc, and zinc interstitials and related defects in lasers with high zinc contents.

Die Mikrostruktur degradierter GaInAsP/InP-Heterostruktur-Laserdioden mit vergrabenen elektrooptischen Schichten wird in Lasern mit niedrigen und mit hohen Zinkdotierungsgehalten des p-InP Begrenzungsbereiches untersucht. Die Mikrostruktur wird mit den jeweiligen Zeitkurven der Schwellenstromwerte korreliert. Versetzungen, die schon vor den Überstreß-Lebensdauertesten gegenwärtig waren, initiieren die Degradation, wohingegen die strukturellen Eigenschaften und die Degradierungsgeschwindigkeit von der Art der Punktdefekte, die ursprünglich in den zwei Lasertypen zugegen waren, bestimmt wird. In den Lasern mit niedrigen Zinkgehalten scheinen die letzteren vorwiegend aus Leerstellen der Gruppe III und Zwischengitterstellen der Gruppe V und in den Lasern mit hohen Zinkgehalten aus mit dem Zink verbundenen Zwischengitterstellen und korrelierten Defekten zu bestehen.

1. Introduction

GaInAsP/InP lasers are widely used in optical communication systems and it is therefore of importance to establish what factors influence their reliability. This paper describes studies of early buried heterostructure (BH) lasers which showed variable degradation rates in overstress life tests. The degradation was most manifest as a rapid increase in the lasing threshold current. There are two potential generic mechanisms, both of which give rise to a non-radiative or leakage current. The first is parasitic leakage due to non-radiative recombination in, or close to, the active region. This might have microstructural causes, i.e. defects in or near the active region. The second mechanism is current leakage remote from the active region, i.e. through the current-blocking layers. This would be a majority

[1]) P.O. Box 88, Manchester M60 1QD, United Kingdom.

carrier controlled degradation process, which might be due to enhanced majority carrier capture by defects. In either case, if overstress promotes defect growth in the regions of current flow this will enhance the leakage current giving rise to an increase in the current required to reach the lasing threshold. The degradation rate would be influenced by the content of point defects in the structure which become active as non-radiative recombination centres and which are able to migrate and promote defect growth during operation of the laser.

This paper deals with some aspects of microstructural investigations of degraded BH lasers, believed to contain different types and concentrations of point defects, in order to clarify which of the mechanisms dominates the threshold current degradation.

2. Experimental

The specimens were aged BH laser diodes and unaged controls of the structure shown schematically in Fig. 1. Prior to transmission electron microscopy (TEM) investigations the lasers underwent accelerated life tests at a temperature of 125 °C and a drive current of 100 to 200 mA for durations up to 600 h. At intervals during this time the samples were removed from overstress and their light–current and current–voltage characteristics were measured at a number of temperatures. Two types of lasers using "low" and "high" zinc doping of the p-type InP confining layer in the vicinity of the active region side-walls were studied. For the low zinc-doped devices, regrowth of the confining layers was performed at 650 °C. For the high zinc-doped lasers the initial part of the regrowth was performed at a lower temperature resulting in a higher zinc incorporation in the shaded regions shown in Fig. 1.

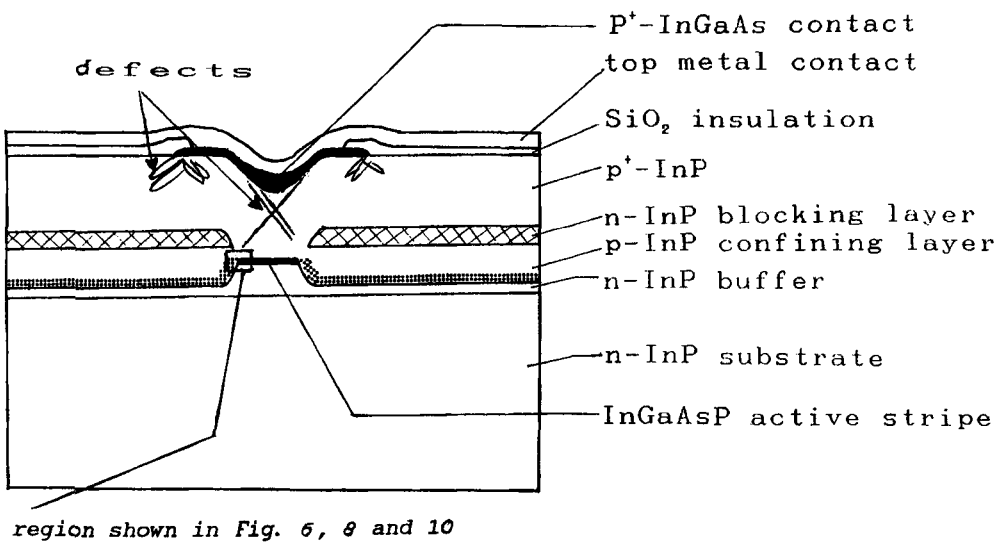

Fig. 1. Schematic diagram of a BH laser section parallel to the facet. Dimensions are typically 100 μm height, 300 μm width, and 400 μm length (extending into the paper). The active stripe is approximately 1.5 μm wide and 0.1 μm high and extends over the length of the laser. Dislocation configurations and nucleation points are sketched in

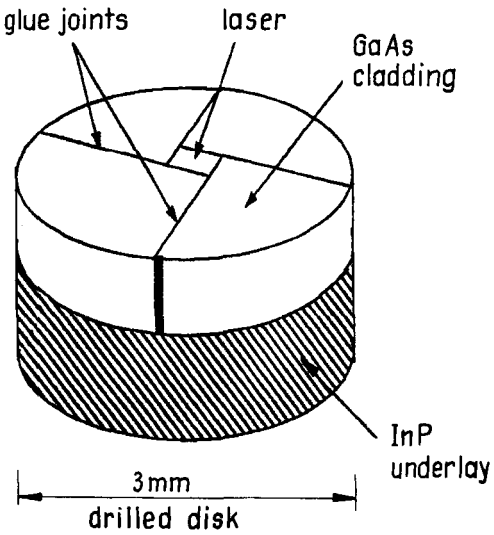

Fig. 2. Geometry of the stack for the preparation of the 3 mm TEM specimen disk

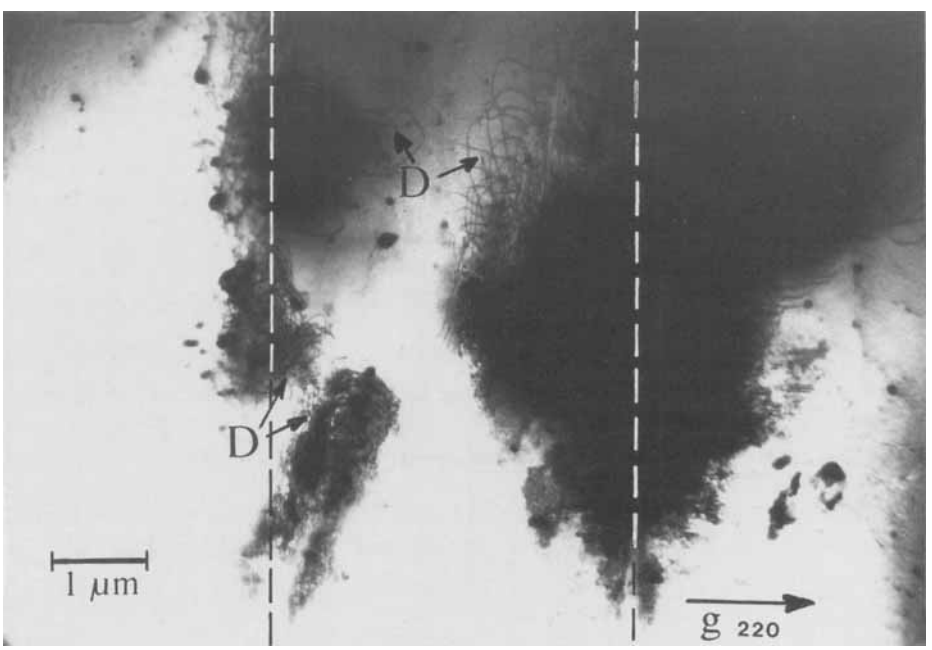

Fig. 3. Plan-view TEM micrograph from the p-InP region of an undegraded laser diode just below the metal contact/oxide. Dislocations (marked D) can be seen to nucleate near the oxide window edges, the former positions of which are indicated by dashed lines. In the very dark regions the specimen still contains a thin residual metal layer originating from the top metal contact

Lasers were sectioned for TEM in a plane parallel or perpendicular to their facets. In both cases the lasers were placed on InP underlay material and surrounded by GaAs cladding material in a close-packed fashion (see Fig. 2). The stack was bonded with M-Bond 600 and a 3 mm disk drilled with the lasers in the centre. In the case of the cross-sectional sample (i.e. the section parallel to the facet) the underlay was then ground off and the whole disk was mechanically polished from both sides down to approximately 60 μm thickness, finishing off with 1 μm diamond polish. Electron microscope copper slot grids were glued onto both sides for support and the sample thinned to electron transparency by Ar-ion milling from both sides at liquid nitrogen temperature. In the case of the section parallel to the top contact ion milling was first performed from the top contact side to a depth just above, or including, the active region (i.e. up to 3 μm down from the top metal contact). The preparation was then continued by mechanically polishing from the back side only, and also the final Ar thinning to electron transparency was only performed from the back side.

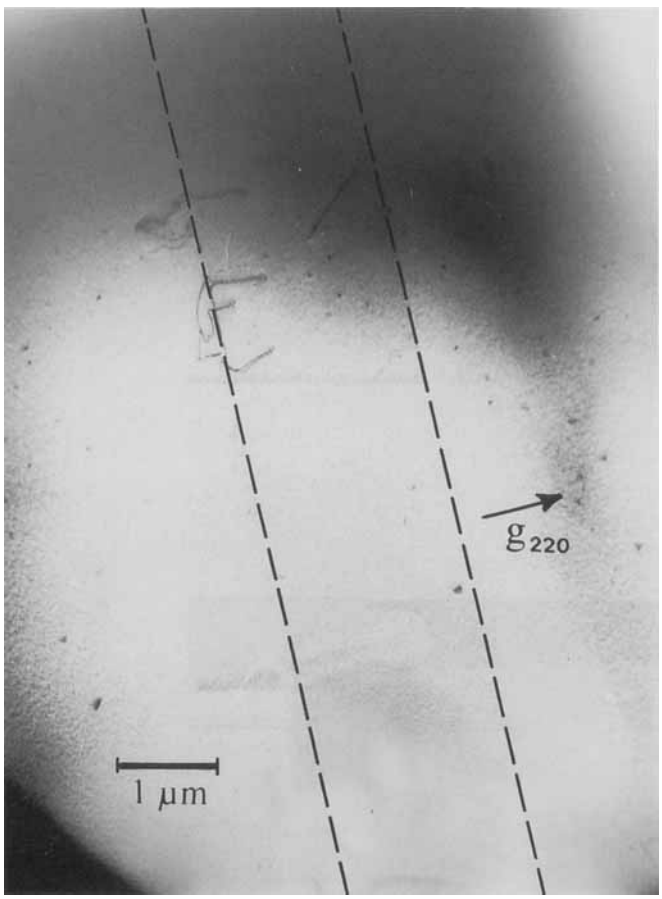

Fig. 4. Plan-view TEM micrograph of a region containing the active stripe indicated with dashed lines in a laser diode of the same type as in Fig. 3. Dislocation segments descending from the top contact/oxide into the p-InP infill layer are pinned at the active region side-wall

TEM studies were undertaken after 4 h life test on low zinc lasers and after 600 h on high zinc lasers, using a Jeol 2000FX operated at 200 kV and low electron beam currents.

3. Results

3.1 Unaged control samples

None of the laser diodes showed any defects due to substrate quality, epitaxial growth or regrown interfaces. The oxide window, however, and also the p^+-GaInAs contact underneath the oxide window, introduced considerable strain in these particular devices and gave rise to dislocation loops and stacking faults penetrating on {111} planes into the device. Fig. 3 shows a plan-view section taken just underneath the top metal contact. Dislocations nucleating in clusters along the edge of the oxide stripe window can be observed. Many of these dislocations do not descend far into the device. This can be observed in Fig. 4, which shows a plan-view section containing the top part of the active region and material above. Most of the dislocations have disappeared, however, some reach the active region. As soon as they intersect the GaInAsP/InP interface their propagation behaviour changes and pinning effects at the active region sidewall can be observed.

The cross-sectional view in Fig. 5 illustrates the above situation further: A segment of a dislocation loop can be seen in the p-InP current-blocking infill layer above the active region. It does, however, not penetrate the quaternary alloy. Also the p^+-GaInAs contact has been observed to give rise to stacking faults or microtwins (see Fig. 9) due to mismatch. There were no defects observed elsewhere in the structure and the blocking layer junctions appear to be of high quality.

The defects originating in the contact region were clearly present before laser operation. They appear never to extend below the active region into the n-InP buffer. Under overstress

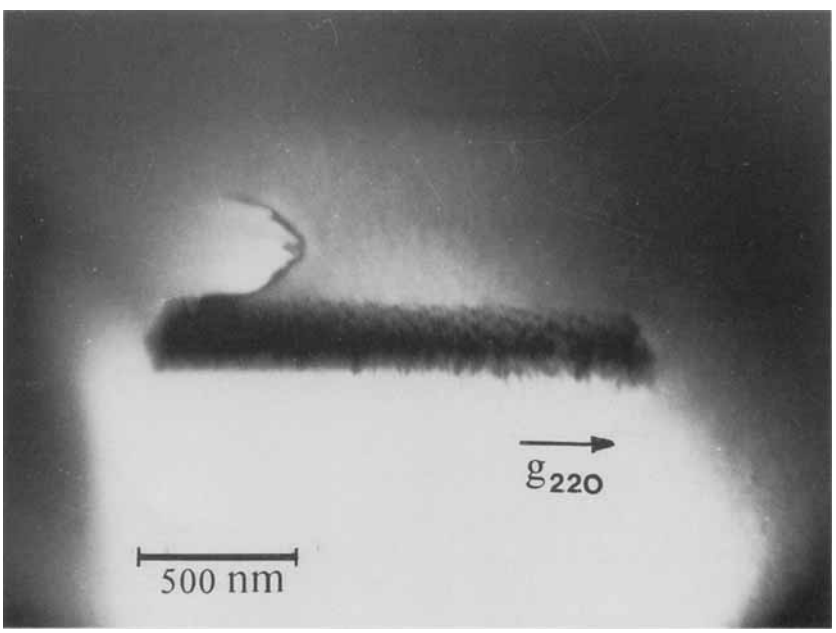

Fig. 5. Cross-sectional view of the active stripe showing a section of a descending dislocation loop in an undegraded laser diode

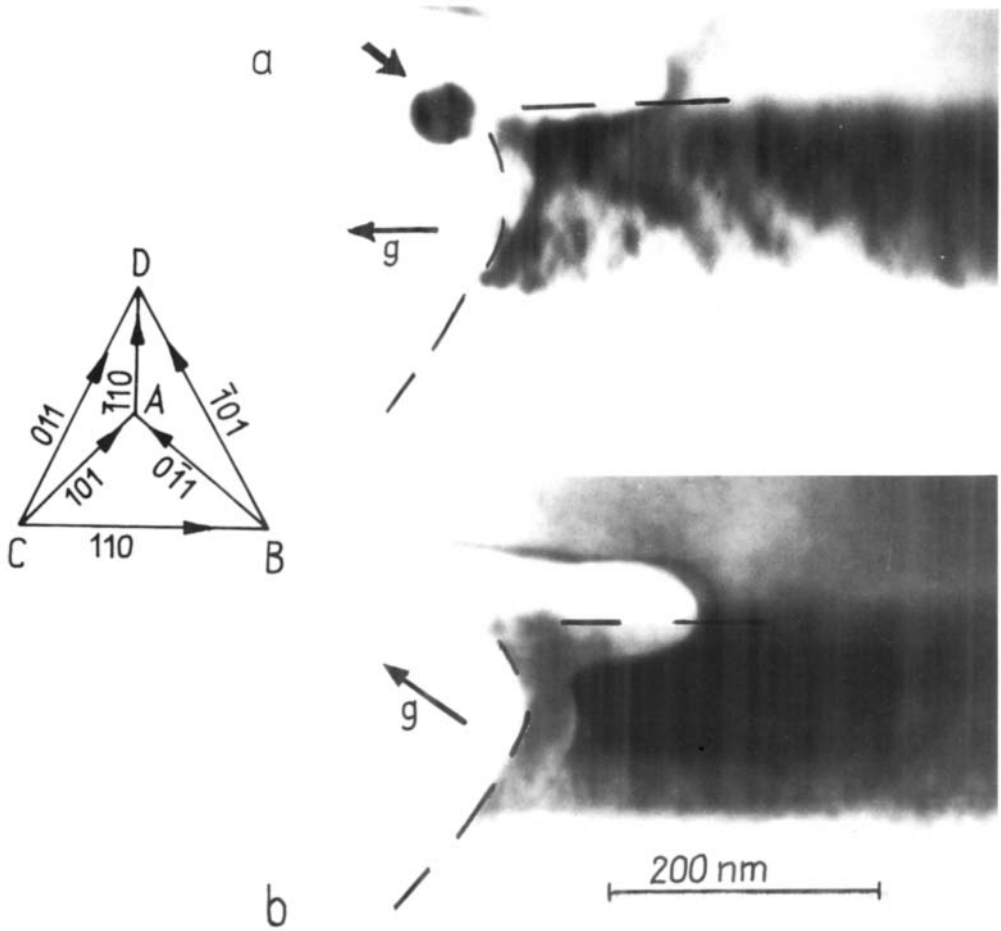

Fig. 6. Cross-sectional view of the active region side-wall of a low zinc laser diode after 4 h overstress test. a) A dislocation loop (arrow) has nucleated on a ABC (or BCD) plane corresponding to the inserted Thompson tetrahedron, $\boldsymbol{g} = [\bar{2}\bar{2}0]$. b) Invisibility condition with $\boldsymbol{g} = [\bar{1}\bar{1}1]$. The position of the junction is indicated by the dashed line

no new dislocations appear to grow down from the contact region, although new defects can be observed to nucleate in the vicinity of the active region and seem to be connected with dislocations present before aging.

3.2 Degradation of lasers with low zinc content

The very large increase in threshold current from typically 13 mA to an average value of 100 mA after 4 h at 125 °C is not reflected, as might be expected, in a marked change in the microstructure. The only features that were observed to be different from unstressed specimens were small dislocation loops of Burgers' vector $(a/2)\langle 101\rangle$ near the active region side-wall (Fig. 6). Tilting experiments show that unlike the dislocations found in unstressed specimens, these defects do not lie on ACD or ABD planes, but on BCD or ACB planes

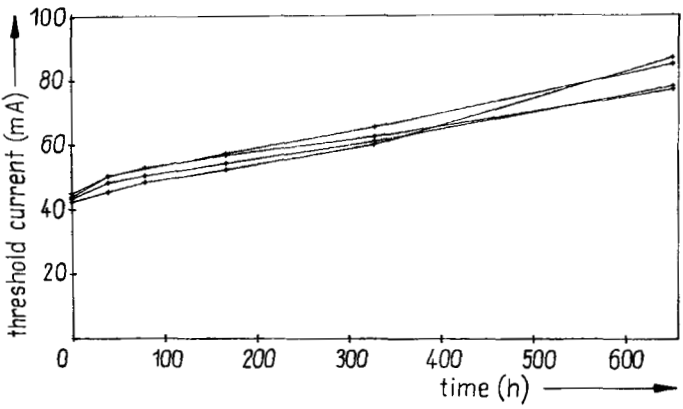

Fig. 7. Threshold current versus ageing time measured for a number of high zinc laser diodes

in the Thompson tetrahedron inserted in Fig. 6. This suggests that the loop might have grown via cross-climb out of a dislocation present before overstress.

3.3 Degradation of lasers with high zinc content

Lasers with high zinc content near the active layer side-wall showed higher threshold currents prior to overstress aging but showed a slower rate of increase during overstress tests (Fig. 7). Thus it took 600 h for the threshold current to increase to a similar magnitude

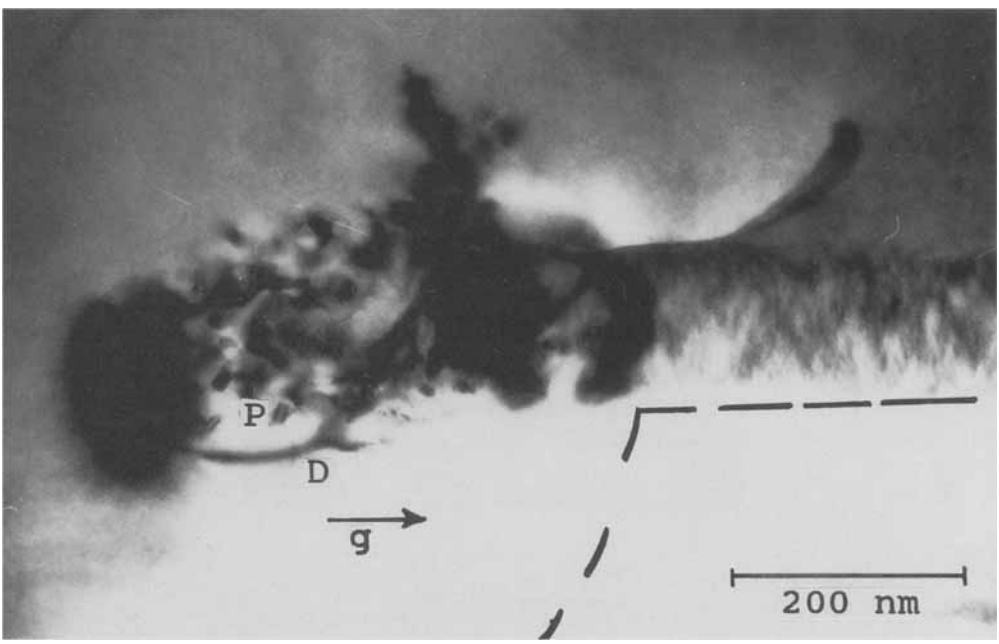

Fig. 8. Cross-sectional view of the degraded active region side-wall in a high zinc laser diode after 600 h ageing, g = [220]. The precipitates (P) exhibit moiré fringes and have punched out a dislocation loop (D). The position of the junction is indicated by the dashed line

to that reached by the low zinc content devices after 4 h subjected to the same current and temperature. This suggests a different degradation process from that found in the low zinc case. The defect structure is in fact remarkably different. Precipitate clusters (P) can be observed to condense out in the vicinity of defects (Fig. 8) similar to the dislocations present before overstress test in Fig. 4 and 5, which, however, are not shown in this figure. The precipitates show a radial distribution with respect to the active region side-wall. This suggests the involvement of point defect diffusion out of the highly-doped junction region, in particular the side-wall. In the strain field of the precipitates new dislocations (point D in Fig. 8) are punched out. The precipitates in Fig. 8 resemble the indium-rich precipitates found in InP samples where loss of phosphorus due to heating has taken place. The extremely high doping level suggests that a considerable fraction of the zinc in the high zinc lasers is present as interstitials. It is suggested by several authors [1, 2] that interstitial zinc diffusion results in production of group-III interstitials (due to a kick-out mechanism), which we believe produce indium-rich precipitates. These observations support the occurrence of zinc diffusion during laser operation.

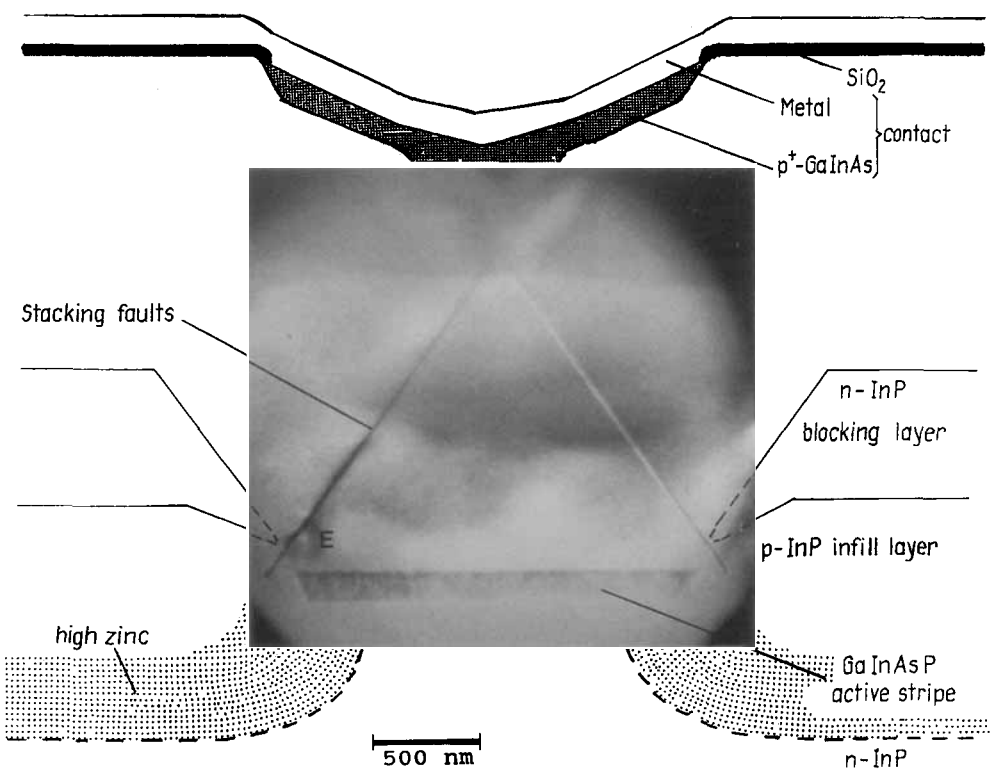

Fig. 9. Cross-sectional view of the active region and top contacts in high zinc laser diode after 600 h overstress test. The stacking fault nucleation at p^+-GaInAs top contact has taken part prior to, and the development of the 'strange' contrast in patch E during laser operation; g = [220]

3.4 Stacking fault reactions

In BH lasers, including the undegraded control samples, it was often found that a series of closely spaced stacking faults on ABD and ACD planes originated at the V-shaped centre of the p^+-GaInAs top contact due to some mismatch with the InP (see sketch in Fig. 1). Fig. 9 shows this situation in a degraded laser: Occasionally these defects descended through several microns of material to the depth of the active GaInAsP stripe. It was observed that they never descended any lower and that their ends were always very close to the active stripe.

Fig. 10 shows a blown-up version of the area around patch E of Fig. 9 in three different reflections. It can be seen from Fig. 10 b and c that in highly zinc-doped lasers large faulted loops on ACD planes have developed near the end of the long stacking fault H, which was there prior to degradation and which is confined by a Shockley partial. In the reflection in Fig. 10 a an additional diffuse contrast patch E appears, which has no discrete dislocation line associated with it. It appears in the region between the edge of the active stripe and the n-InP blocking layer edge (see Fig. 1). X-ray analysis was performed on patch E as well as in other places including the p-InP infill layer and higher parts of the long stacking fault H. Whereas the latter regions showed the expected composition (i.e. InP), patch E revealed a gallium content of $\approx 3.6\%$ and an arsenic content of $\approx 5.4\%$, though none of these elements ought to be present.

4. Discussion

It is clear that the dislocations present before ageing play a key role in the degradation process. It is known that insulating oxides in devices are often under stress and that the strain distribution due to an oxide stripe window adversely affects the lasing performance [3, 4] of GaAs-based lasers. The location of the highest stress is close to the edges of the oxide, where dislocation loops are nucleated. Due to misfit with the InP, the p^+-GaInAs contact is another source of defects. Fig. 9 shows that the interface between the GaInAs and the InP is grooved with the planes of the grove close to $\{111\}$. The grove planes have become the growth planes of the GaInAs. It is known that 111-growth facilitates stacking fault and microtwin formation. With adequate changes of the contact geometry, it should be possible to prohibit the formation of these defects.

In overstressed devices, no evidence for the growth of new dislocations from the top contact downwards has been observed. Nor is there evidence for defects or dislocations in the blocking layers which might cause current leakage.

The climbed dislocation loops in the active layer side-walls, shown in Fig. 6, suggest that point defects, i.e. vacancies or interstitials, must be present near the active layer junction. These loops form only during operation and it is hence reasonable to assume that point defect diffusion is initiated by recombination enhanced defect reactions (REDR). These point defects then condense out on dislocations which were present before ageing and which are now able to climb. The formation of group-III vacancies (several times 10^{17} cm^{-3}) and group-V interstitials is a known phenomenon in MOCVD growth. Hence dislocation climb can happen via either of these types of point defects. O'Hara et al. [5] have observed that dislocations in GaAs climb by consumption of interstitials and emission of vacancies. Group-V interstitials have a low migration energy and it is therefore likely that they are similarly responsible for dislocation climb in our low zinc lasers during operation.

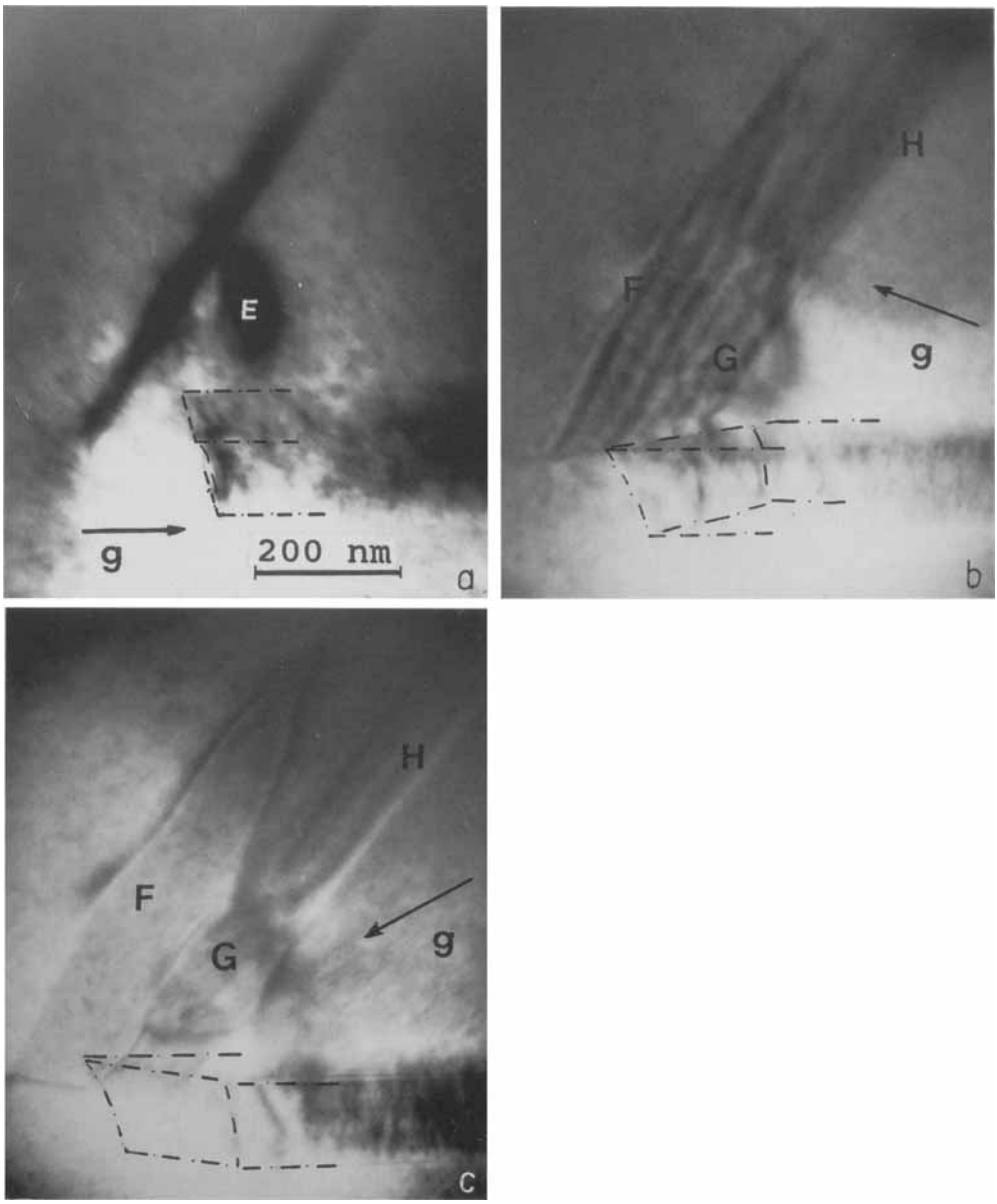

Fig. 10. a) Enlarged area around patch E in Fig. 9; $\boldsymbol{g} = [220]$. b) and c) show same area at high tilts with $\boldsymbol{g} = [\bar{2}\bar{4}2]$ and $\boldsymbol{g} = [\bar{2}\bar{2}\bar{4}]$, respectively, revealing faulted loops F and G close to the bottom part of and parallel to stacking fault H. Patch E appears as residual contrast. The dashed-dotted line indicates the active region interfaces

This results in the formation of small loops. The threshold current increase suggests that the new defects act as non-radiative recombination centres. The energy dissipated by non-radiative recombination promotes more point defect diffusion which in turn creates more defects acting as non-radiative recombination centres. The steep increase of the threshold current value suggests an escalating process, which is in agreement with the mechanism outlined above.

We also conclude that the threshold current increase is not due to leakage through the blocking layers remote from the active region, but is due to non-radiative losses in the active region side-wall.

In the case of the lasers highly-doped with zinc, the rate of threshold current decreases initially on overstress, then, after some hours of operation it increases again, resulting in a slight supralinearity of the threshold current versus time curve (Fig. 7). It appears that two processes are competing here. The initial decrease in the rate of threshold current indicates an outward diffusion of some kind of point defect away from the junction. This defect then does not play any further role in recombination enhanced processes. We suggest that recombination enhanced zinc diffusion is taking part initially. Zinc diffusion is a favoured and well-documented process in InP and related compounds [6 to 8]. In the lasers it will have two effects: firstly, it moves the p–n junction into the n-doped region. A displacement of the p–n junction has been observed in scanning electron micrographs obtained on etched laser facets (ATR Briggs, BNRE private communication). The approximate position of the junction is sketched as dashed line in Fig. 8. (Similarly in Fig. 6 the dashed line indicates the junction in low zinc-doped lasers.) Secondly, zinc diffusion promotes defect formation, e.g. precipitation at the diffusion front [9]. A radial distribution of precipitates with respect to the active region side-wall can be observed in Fig. 8. The precipitates form remote from the junction and hence do not take part in REDR. This is in agreement with the observed initial decrease in the rate of the threshold current. After zinc diffusion has slowed down, loop formation (as in the low zinc lasers) picks up. A proportion of group-V interstitials is likely to have been used up in precipitate formation [9] and hence loop formation via climb will take place at a lower rate in the low zinc samples. This assumption agrees with the slow supralinear increase in the threshold current curve in Fig. 7.

The zinc diffusion will preferably go in two directions, into the quaternary layer, where the solubility is higher than in InP [7] and into the n-doped InP blocking layers. The diffusion front will leave a trail of disorder [2, 9, 10, 11], e.g. vacancies, group-III interstitials, and possibly antisite defects behind. Most importantly it has been found by van Gurp et al. [11] that substantial mixing of the gallium and the indium in the vicinity of InP/GaInAsP junctions due to zinc diffusion can take place. This would explain the gallium in patch E in Fig. 9 and 10a, which migrates out of the active stripe as part of the point defect trail behind the zinc diffusion front. Furthermore the zinc diffusion in these lasers also appears to affect As/P intermixing.

The nucleation of the faulted loops F and G on the ABD plane could have involved the Shockley partial of the near by stacking fault H. The growth of dislocations from Shockley partials during laser operation in GaAs lasers has been reported by Ito et al. [12]. Burgers vector analysis (see visibility/invisibility in Fig. 10 b, c) shows that loops F and G are Frank partials with Burgers' vector $\boldsymbol{b} = (1/3)\,[1\bar{1}1]$. Frank partial loops grow by the process of climb requiring point defects. There is extensive literature on gettering and decoration due to point defect diffusion in the vicinity of the dislocations, which confine stacking faults

[13]. There appears to be a plentiful supply of point defects near patch E, which proved rich in Ga and As. These can be expected to diffuse readily along the stacking fault, leading to decoration (loops F and G), starting at the Shockley partial and proceeding upwards alongside the stacking fault. This can be seen in Fig. 10b and c.

Finally, it should be mentioned that microstructural degradation is predominantly observed in the p-type InP region and not in the GaInAsP active region, which appears to be fairly resistant to penetration by dislocations.

5. Conclusion

In conclusion it can be said that recombination enhanced point defect diffusion into the p-type InP near the active junction is believed to control the threshold current increase in aged BH GaInAsP/InP lasers. The consequence is the formation of defects, containing non-radiative recombination centres, out of dislocations present before ageing. This results in further non-radiative losses.

The defect type and the speed and characteristics of the degradation process are determined by the type of point defect and are substantially different in lasers with an abundance of intrinsic defects (group-V interstitials/group-III vacancies) or with zinc interstitials. The former lead to the formation of small perfect loops and a rapid increase in threshold current, the latter lead to numerous larger precipitates, outdiffusion of Ga and As out of the active region along stacking faults, and decoration of the latter. The threshold current increase is overall smaller than in the first case. This is believed to be due to the activity of the different type of point defect and the remoteness of the operating junction from the defects.

Acknowledgements

The work was partly carried out on an Advanced SERC Fellowship (ITF/189, U.B.). We also thank C. Dieker from the Forschungszentrum Jülich for help with the X-ray analysis.

References

[1] V. GOESELE and F. MOREHEAD, J. appl. Phys. **52**, 4617 (1981).
[2] M. LUYSBERG, W. JAEGER, K. URBAN, M. PERRET, N. A. STOLWIJK, and H. MEHRER, Inst. Phys. Conf. Ser. No. 100, 409 (1989).
[3] M. J. ROBERTSON and B. WAKEFIELD, J. appl. Phys. **52**, 4462 (1981).
[4] A. FRIED, A. JAKUBOWICZ, S. B. NEWCOMB, and W. M. STOBBS, Inst. Phys. Conf. Ser. No. 117, 585 (1991).
[5] S. O'HARA, P. W. HUTCHINSON, and P. S. DOBSON, Appl. Phys. Letters **30**, 368 (1977).
[6] F. C. FRANK and D. TURNBULL, Phys. Rev. **104**, 617 (1981).
[7] G. J. VAN GURP, P. R. BOUDEWIJN, M. N. C. KEMPENERS, and D. L. A. TJADEN, J. appl. Phys. **61**, 1846 (1987).
[8] G. J. VAN GURP, D. L. A. TJADEN, G. M. FONTIJN, and P. R. BOUDEWIJN, J. appl. Phys. **64**, 3468 (1988).
[9] P. W. HUTCHINSON, P. S. DOBSON, B. WAKEFIELD, and S. O'HARA, Solid State Electronics **21**, 1413 (1978).
[10] K. BALL, P. W. HUTCHINSON, and P. S. DOBSON, Phil. Mag. **A43**, 1299 (1981).
[11] G. J. VAN GURP, W. M. VAN DE WIJGERT, G. M. FONTIJN, and P. J. A. THIJS, J. appl. Phys. **67**, 2919 (1990).
[12] R. ITO, H. NAKASHIMA, and O. NAKADA, Japan. J. appl. Phys. **13**, 1321 (1974).
[13] F. G. KUPER, J. T. M. DETTOSSON, and J. F. VERWEY, Inst. Phys. Conf. Ser. No. 76, 495 (1985).

(Received February 17, 1993)